A micro dew point sensor with a thermal detection principle

M Kunze[1], J Merz[1], W-J Hummel[2], H Glosch[1], S Messner[1] and R Zengerle[1,3]

[1] HSG-IMIT—Institut für Mikro- und Informationstechnik der Hahn-Schickard-Gesellschaft eV, Wilhelm-Schickard-Street 10, 78052 Villingen-Schwenningen, Germany
[2] IL Metronic Sensortechnik GmbH, Mittelstraße 33, 98693 Illmenau-Unterpörlitz, Germany
[3] Laboratory for MEMS Applications, Department of Microsystems Engineering (IMTEK), University of Freiburg, Georges-Koehler-Allee 106, 79110 Freiburg, Germany

E-mail: michael.kunze@hsg-imit.de

Abstract
We present a dew point temperature sensor with the thermal detection of condensed water on a thin membrane, fabricated by silicon micromachining. The membrane ($600 \times 600 \times \sim 1\ \mu m^3$) is part of a silicon chip and contains a heating element as well as a thermopile for temperature measurement. By dynamically heating the membrane and simultaneously analyzing the transient increase of its temperature it is detected whether condensed water is on the membrane or not. To cool the membrane down, a peltier cooler is used and electronically controlled in a way that the temperature of the membrane is constantly held at a value where condensation of water begins. This temperature is measured and output as dew point temperature. The sensor system works in a wide range of dew point temperatures between 1 K and down to 44 K below air temperature. In experimental investigations it could be proven that the deviation of the measured dew point temperatures compared to reference values is below ± 0.2 K in an air temperature range of 22 to 70 °C. At low dew point temperatures of -20 °C (air temperature = 22 °C) the deviation increases to nearly -1 K.

(Some figures in this article are in colour only in the electronic version)

1. Introduction

The continuous optimization of technical processes, their permanent control as well as the growing demand on the quality of products and the trend toward energy efficiency lead to an increasing demand for all kinds of sensor solutions for the control of technical processes. In many application fields where air or other gases are needed and used, humidity is an increasingly important parameter. In technical processes and equipment especially absolute humidity, which is the content of water vapor in air, is often more relevant than relative humidity (RH). A definition and explanation of the different quantities used to express humidity is given in [1]. To determine absolute humidity dew point temperature can be measured. The dew point temperature is the temperature where condensation and evaporation of water is at equilibrium.

It can either be calculated from RH and gas temperature or is directly measured using for example chilled mirror dew point meters.

Beside some others, there are in general two different types of humidity sensor principles. Adsorption-type sensors are based on the effect that depending on RH and temperature of a gas the amount of water molecules inside a material varies. As a result, a certain parameter of the material changes. An example of such sensors is the widely used capacitive humidity sensors where the permittivity of for example a polymer and consequently the measured sensor capacity changes with the amount of incorporated water molecules.

Condensation-type humidity sensors are based on the effect that water molecules condense onto a cooled surface at dew point temperature. These types of sensors directly measure dew point temperature and hence absolute humidity.
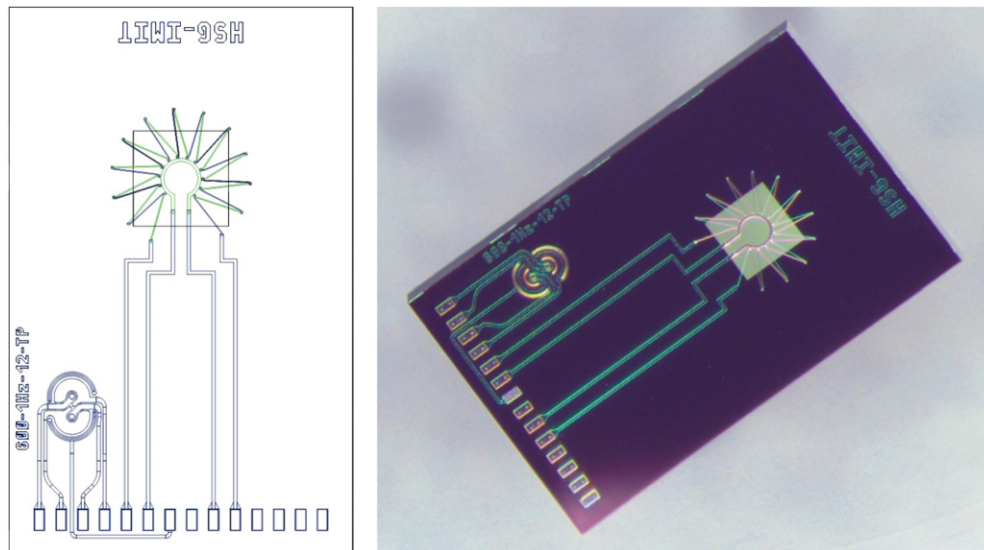
Figure 1. Layout (left) and photograph (right) of the silicon sensor chip. The diode for absolute temperature measurement is placed in the lower left corner. The membrane with ring-shaped heating element and circular arranged thermopiles can be seen in the center of the upper half of the chip.

Chilled mirror dew point meters are such devices and are mostly used in laboratory applications. The principle relies on the gradual cooling of a body (normally a mirror). Due to the cooling of the body, the surrounding air or gas will also be cooled until the dew point temperature is reached. At this temperature, water condenses at the surface of the body (mirror) which is typically detected by optical means [2]. The temperature at which condensation appears is defined as the dew point temperature.

In total, a lot of different approaches to measure either relative or absolute humidity were examined in the past [3, 4]. In [5, 6] various concepts to realize humidity sensors using micromachining or MEMS (micro electro mechanical system) technologies are presented. A MEMS dew point temperature sensor based on a similar concept as the presented sensor, but using capacitive detection of condensed water, is presented in [7]. Two examples of MEMS-based humidity sensors which are already established on the market are offered by the company Sensirion [8] and by CIS Institut für Mikrosensorik [9].

In this paper, we present a MEMS-based dew point temperature sensor which relies on the thermal detection of condensed water on a cooled thin membrane. The basic feasibility of the sensor principle and first results of the complete sensor system were presented earlier in [10, 11]. New measurement results prove that the sensor system works with good precision in the range below 10% RH as well as at high humidity values of up to nearly 96% RH at elevated air temperatures of up to 70 °C.

2. Concept and design

The concept of the condensation-type humidity sensor with thermal detection principle described in this paper is based on the fact that the specific heat capacity as well as enthalpy of evaporation of water is high. Due to these properties a

relatively high amount of energy is needed to warm up and finally evaporate even small amounts of water. This means that the temperature of a dry body which is heated with defined power will increase faster compared to a body with condensed water on its surface. This effect is used to detect condensation in our sensor system and gets more efficient with decreasing mass and heat capacity of the body. Because MEMS technology offers means to fabricate structures with low heat capacity as well as integrated heating elements and temperature sensors, this technology was used to realize the sensor.

The key element of our condensation-type humidity sensor is a membrane ($600 \times 600 \times \sim 1\ \mu m^3$) made of Si_3N_4 and SiO_2 offering a very low heat capacity and a very low heat conductivity [12]. A central ring-shaped heater made of poly-silicon allows the heating of the membrane. Circular arranged thermocouples connected in series (thermopile) made of poly-silicon and aluminum detect the temperature difference (ΔT_{MB}) between the membrane and the silicon bulk material (figure 1). A diode located in the silicon bulk material is used to measure the absolute bulk temperature (T_B). The surface of the sensor chip is coated with SiO_2 and Si_3N_4 to protect the heater, thermopile and diode against aggressive media.

The membrane is cooled using a peltier cooler, which is positioned underneath the membrane (figure 2). For proper function of the sensor it is essential that without heating it, the membrane is the coldest spot of the sensor chip and that there is a temperature difference from the silicon bulk material. To achieve this temperature difference, a special coupling chip made of silicon is positioned between the sensor chip and the peltier cooler. The outer frame of the coupling chip is mounted on the silicon bulk of the sensor chip, using a thermally insulating adhesive so that the thermal resistance in this area is high. The embossed area in the middle of the coupling chip is positioned exactly underneath the membrane with a clearance of approximately 50 μm. Experimental investigations proved
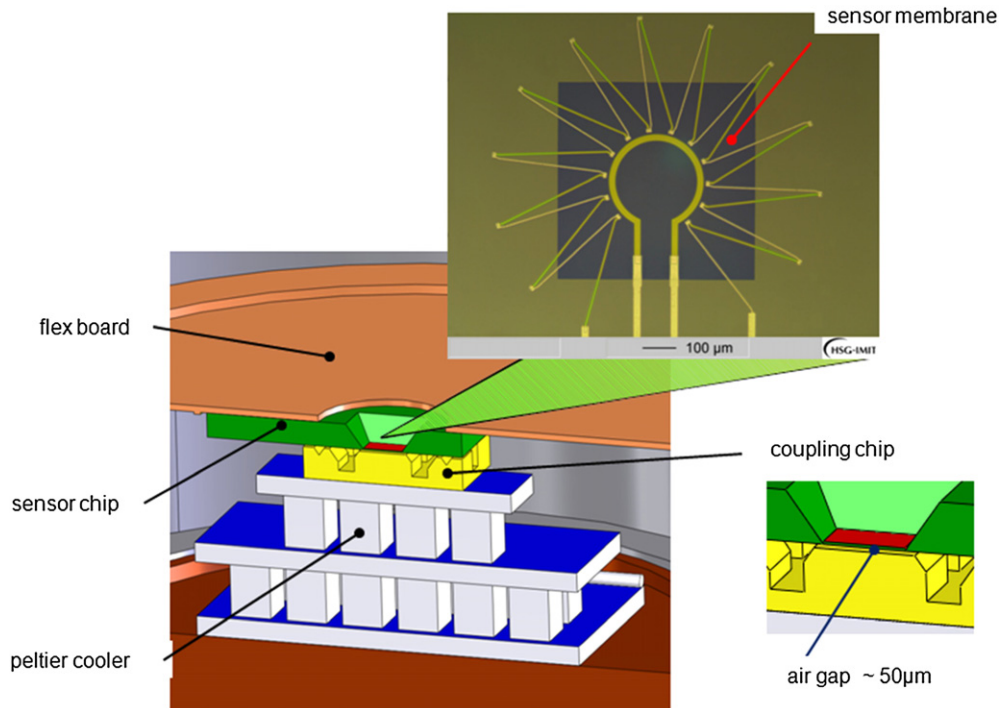
Figure 2. Detailed view of the sensor system assembly showing silicon sensor chip, coupling chip, peltier cooler and flex board.

that the heat transfer over this air gap is sufficient to achieve that the membrane (without heating it) is at least 0.5 K colder than the silicon bulk material.

When a heating pulse of 10 mW is applied to the membrane for 50 ms, the increase in temperature difference between membrane and silicon bulk material ($\Delta T_{MB} \approx 60$ K within ~15 ms) is dynamically recorded using the thermopile (figure 3, circles). The variation of temperature difference with time is characteristic for the heat capacity of the membrane. When the membrane is cooled slightly (approximately 0.1–0.2 K) below dew point temperature, water condenses on the membrane (figure 4). The condensed water on the membrane and its heat capacity, respectively, lead to a slower increase of temperature difference between membrane and silicon bulk material (figure 3, triangles). The difference of both curves is calculated and integrated over a period of 25 ms. The resulting integration value (absolute value of the hatched area shown in figure 3) is a measure for the amount of condensed water on the membrane and its heat capacity, respectively.

According to experimental investigations the best performance is achieved when a condensation phase of 2 s is followed by two heating pulses of 50 ms with a time-lag of 60 ms in between. With the first heating pulse the thermal response of the membrane with or without condensed water is recorded. If condensed water was on the membrane before the first pulse, the heating power is sufficient to evaporate it. This leads to a dry membrane after the first heating pulse. The time-lag to the second pulse (60 ms) is too short for significant re-condensation of water. Hence, with the second heating pulse, the thermal response of the dry membrane can be recorded and is used as reference.

If the membrane temperature is above dew point temperature during condensation phase, the difference in both
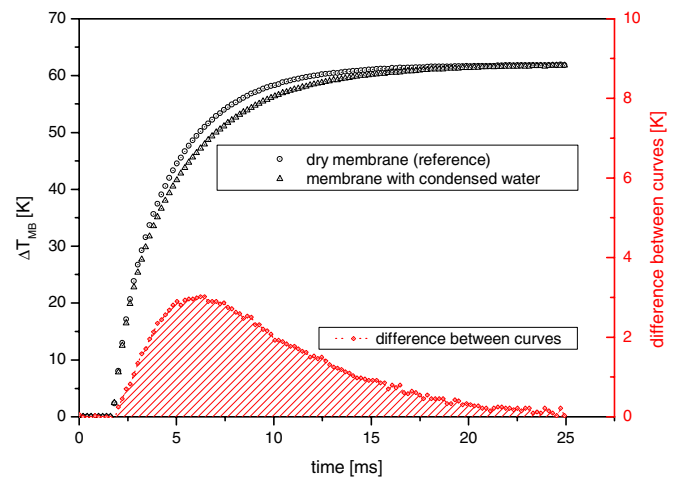
Figure 3. Transient signal measured using the thermopile (temperature difference between membrane and silicon bulk ΔT_{MB}). The circles show the temperature increase of a dry membrane (above dew point temperature) after a heating pulse (10 mW, 50 ms). The thermopile signal of a membrane with condensed water (below dew point temperature) is represented by the triangles. The diamonds show the differences between the measurement values of the dry membrane and the membrane with condensed water on it (right-hand scale).

temperature curves is low and results in a small integration value. In contrast, if the membrane temperature is below dew point temperature and water condenses, there is a significant difference in the two curves (figure 3, diamonds). The integration value increases depending on the amount of condensed water on the membrane. During operation of the sensor, the integration value is recorded while the membrane is continuously cooled down by the peltier cooler. The dew point

3

droplet diameter < 1 μm
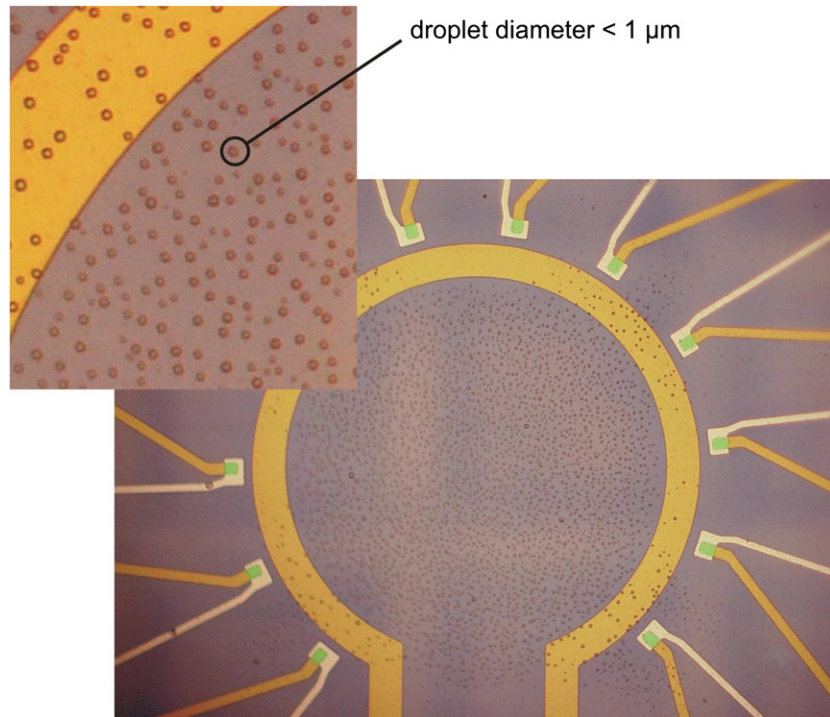
Figure 4. Photograph (detailed view) of a sensor membrane with condensed water droplets (dew) on its surface. The diameter of the droplets is below 1 μm.
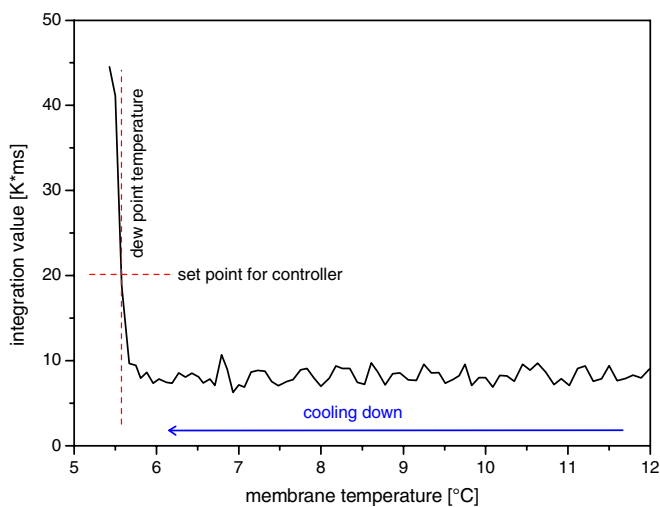
Figure 5. Integration value depending on the temperature of the membrane. The integration value increases significantly when the dew point temperature is reached and water begins to condense on the sensor membrane. For the controller electronics the set point of the integration value was defined to 20 K ms. For the depicted example the dew point temperature at set point is about 5.5 °C.

is reached when water begins to condense on the membrane and hence the integration value starts to increase significantly (figure 5).

As it is not possible to exactly determine the dew point temperature from the curve progression shown in figure 5, a threshold (set point) for the integration value was defined to 20 K ms, based on experimental investigations. The absolute membrane temperature at this set point is the dew point temperature detected by the sensor. This temperature is calculated from the temperature difference between membrane and silicon bulk ΔT_{MB} (measured using the thermopile) and the silicon bulk temperature T_B (measured using the diode). To achieve a fast response of the sensor to changes in RH and dew point temperature, respectively, the membrane is kept at dew point temperature during operation. This is achieved by a two-position controller implemented in microcontroller electronics. It drives the peltier cooler in a way that the integration value is continuously kept at set point. Besides, the microcontroller electronics controls the heating element on the membrane and records the signals from the thermopile and diode.

3. Fabrication

In the following the main steps and processes for the fabrication of the complete sensor system are described focusing on silicon sensor chip and assembly.

3.1. Silicon sensor chip

For fabrication of the silicon sensor chips a double side polished (1 0 0)-oriented n-doped 4″ silicon wafer with a thickness of 380 μm and a resistivity of 2–10 Ω cm is used. First of all, the diode for absolute temperature measurement is fabricated on the top side (TS) of the wafer at an external vendor using standard processes such as pre-deposition diffusion of boron and phosphorus as well as p-implantation of boron (figure 6(a)). After stripping all remaining mask layers from diode fabrication, the process
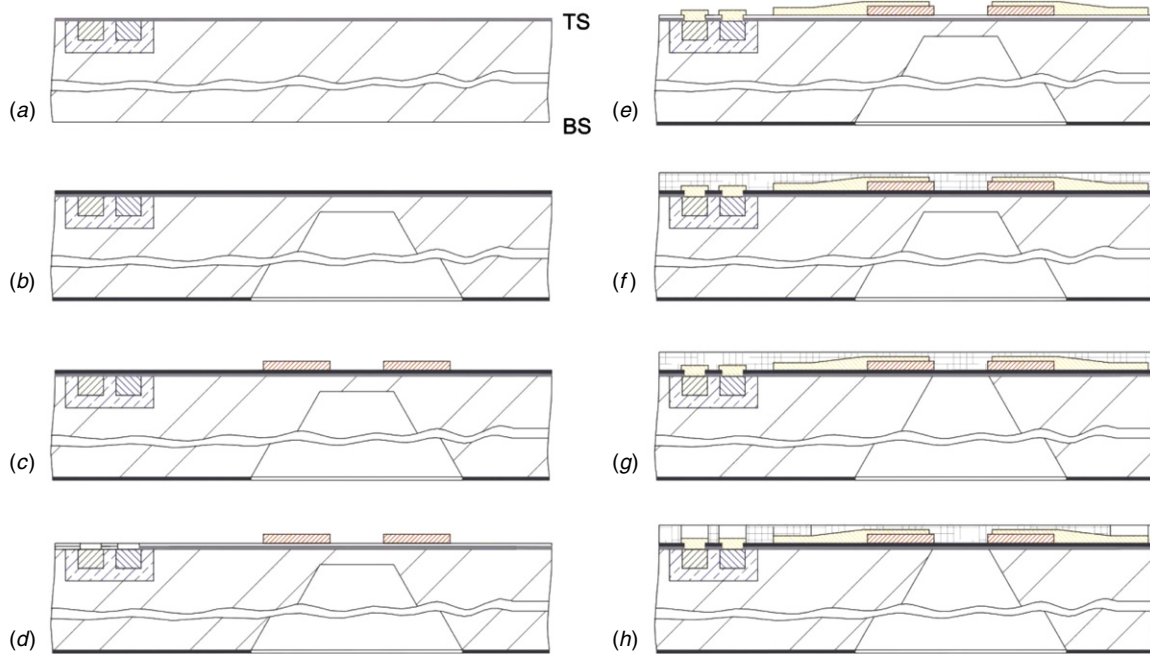
Figure 6. Schematic drawing of the process sequence for the fabrication of the silicon sensor chip.

steps to manufacture the sensor membrane with heating element and thermocouple follow.

In the first step the wafer is coated with a SiO_2 layer followed by a layer of Si_3N_4 (figure 6(*b*)). The coating system acts as a mask for the following wet-etching. After coating the back side (BS) of the wafer with photo resist, the structures of the first mask are exposed to the BS. In the following step the Si_3N_4 layer is removed in the exposed area by dry-etching. After removing the photo resist the SiO_2 layer is wet-etched. A 33% potassium hydroxide solution (KOH) at 80 °C is used to etch the structures of the first mask approximately 330 μm into the BS of the silicon wafer (figure 6(*c*)). In the next step the TS is coated with *in situ* n-doped poly-silicon. After that, a photolithography step using the second mask on the TS follows. In the exposed areas the poly-silicon is removed by dry-etching (figure 6(*c*)). The resulting structures are the heating element and one part of the thermocouples, respectively. After removing the remaining photo resist, a photolithography process using the third mask follows. To open vias for contacting the diode in the following step, the double layer of Si_3N_4 and SiO_2 is removed in the exposed area (figure 6(*d*)). After stripping the photo resist, aluminum (Al) is sputtered to the TS of the wafer. Again, photo resist is applied to the TS of the wafer and the fourth mask is exposed. The remaining photo resist is used as mask for wet-etching the Al layer (figure 6(*e*)). The resulting Al structures are used as second part of the thermocouples, conducting paths and bond pads. To protect the sensor chips against aggressive media, the TS of the wafer is coated with a double layer of SiO_2 and Si_3N_4 (figure 6(*f*)).

After that, the KOH wet-etching of the BS is continued until the buried SiO_2 layer is reached (figure 6(*g*)). In the following step the TS is again coated with photo resist and the fifth mask is used in a photolithography step followed by

removal of the Si_3N_4 and SiO_2 double layer in the exposed areas (figure 6(*h*)). This step is needed to open the bond pads. After stripping the photo resist, the wafer is finally diced into single sensor chips.

3.2. Assembly of the sensor system

The assembly of the sensor system starts with bonding the coupling chip (see figure 2) on the TS of the sensor chip using adhesive. The coupling chip is made of silicon and fabricated by KOH etching and sawing. The sensor chip with bonded coupling chip is then bonded onto the surface of a flex board, which has an orifice in the area of the sensor membrane (figure 7). Through this orifice the air or gas to be measured gets in contact with the sensor. For measurements at elevated pressures, the sensor membrane needs to be pressure balanced. This is achieved by including another orifice in the flex board, so that the pressure applied to the system works on both sides of the sensor chip and membrane, respectively. The flex board further contains conducting paths to electrically connect the sensor chip with the electronics. To electrically contact the sensor chip to the flex board, wire bonding is used. The flex board is also used to thermally decouple the sensor chip from the sensor housing. At this step of the assembly process, the calibration of the diode for absolute temperature measurement takes place. This is a very important step, since the accuracy of the absolute temperature measurement directly influences the accuracy of the sensor system. For calibration a liquid comparison bath and a precision thermometer (ISOTECH, Hydra Model 798 and TTI-7+, respectively [13]) are used resulting in a temperature calibration precision of ± 0.01 K.

The sensor head (see figure 7) is made from high-grade steel and contains contact pins, which are called glass feed-throughs. The advantage of this technology is that glass
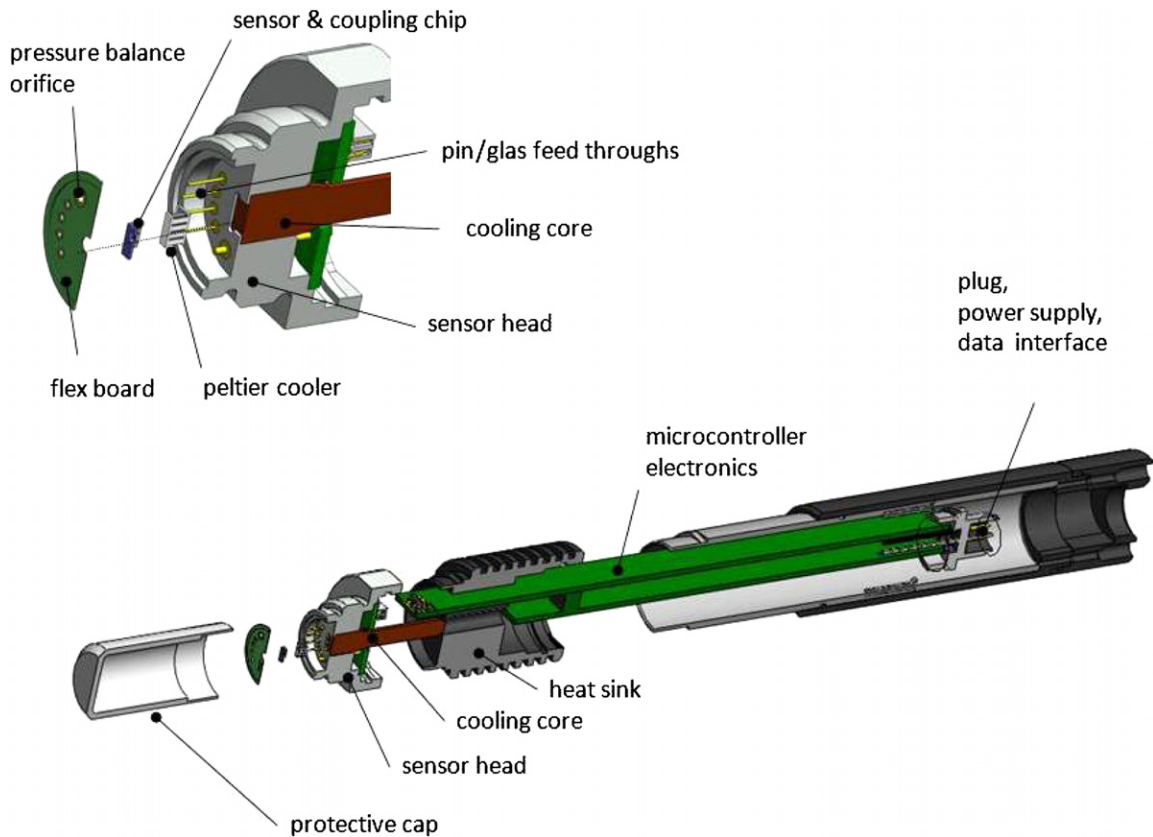
Figure 7. Exploded sectional view of the sensor system showing the assembly of the different components.

feed-throughs are hermetically tight and pressure-resistant. After soldering the so-called cooling core made of copper into the sensor head, a peltier cooler is mounted on the surface of the cooling core. The cooling core can be connected to a heat sink which is needed to cool the warm side of the peltier cooler. In the next step the peltier cooler is connected by soldering wires to contact pins.

Now, the flex board with sensor and coupling chip is mounted to the sensor head, using adhesive technology. By soldering, conducting paths on the flex board and glass feed-through contact pins are electrically connected. In the next step a printed circuit board (PCB) is mounted onto the sensor head. This PCB is used as an adapter board containing a socket for contacting the microcontroller electronics which is needed to drive the heating element on the sensor membrane, record and analyze the sensor signals, and control the peltier cooler. The resulting module can be integrated in further steps into different housings, depending on the specific application (figure 8).

4. Experimental results

In the following, measurement results from characterization in the range of high RH and at elevated air temperatures as well as at low dew point temperatures are presented. The sensor system was designed to also measure at higher pressures. In first experiments it could be proven that the sensor system in principle is able to measure in a pressure range of up to 800 kPa. However, since there was no sensor for reference

measurements at higher pressures available in our lab, the sensor system could not be characterized properly. Therefore, no measurement results at higher pressures are presented in this paper. Since for some applications also response time is an important parameter, characterization results regarding the dynamic behavior of the sensor system are presented at the end of this section.

4.1. Characterization at high humidity and high temperatures

In a first measurement the sensor system was characterized at dew point temperature in the range of 3 to 1 K below air temperature which was set to 25 °C (figure 9). This corresponds to RH values of approximately 83.5% RH, 88.7% RH and 94.2% RH, respectively. The RH values were calculated from the dew point temperatures using the Magnus formula [15]. To generate precisely defined RH values at the defined air temperature, a high quality humidity generator (Thunder Scientific Type 2500 [14]) was used.

To investigate the repeatability of the sensor system, measurements at different dew point temperatures were carried out according to the procedure described in the following. The air temperature was constantly set to 25 °C. The dew point temperature of the air was set to 22 °C (~83.5% RH), then increased to 23 °C (~88.7% RH) and finally to 24 °C (~94.2% RH). After that the dew point temperature was decreased back to 23 °C and finally to 22 °C. This procedure was repeated three times. It can be seen from figure 9 that the reference dew point temperatures vary slightly

Figure 8. Photograph of the realized sensor system. The sensor system on the right is portable and intended to measure in free atmosphere. The sensor system can be equipped with an adapter shown on the left. This adapter contains a quick connect for connecting the sensor system to and measuring in tubing systems. An exhaust throttle allows gas to flow through the connected adapter.
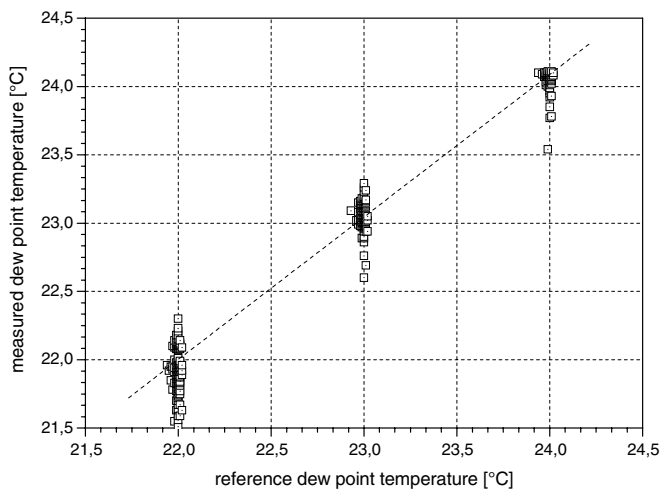
Figure 9. Measured dew point temperature compared to reference values. Humid air was generated using a humidity generator (Thunder Scientific Type 2500 [14]) at an air temperature of 25 °C. The reference dew point temperatures on the *x*-axis are calculated from the actual RH values output by the humidity generator using the Magnus formula [15].

Figure 10. Measured dew point temperature compared to reference values. Humid air was generated using a humidity generator (Thunder Scientific Type 2500 [14]) at an air temperature of 25, 50 and 70 °C. The reference dew point temperatures on the *x*-axis are calculated from the actual RH values output by the humidity generator using the Magnus formula [15]. On the right axis the deviation between measured and reference dew point temperatures is shown.

with a standard deviation of ±0.01 °C around the intended values. Each dew point temperature value was kept constant for 3 h. The sensor system measured every 2 s. Every 100th measurement value is shown in figure 9.

At a dew point temperature of 22 °C the mean of the dew point temperatures measured using the sensor system was 21.99 °C with a standard deviation of ±0.14 °C. The corresponding values for dew point temperatures of 23 and 24 °C are 23.07 ± 0.08 and 24.07 ± 0.07 °C. These results indicate the good accuracy of the sensor system in the range of high air humidity. Furthermore, no significant hysteresis could be recognized by analyzing the measurement results.

To investigate the behavior of the sensor system at higher air temperatures, measurements at 25 °C were compared to measurements at 50 and 70 °C. At each air temperature, dew

point temperatures of 15, 3 and 1 K below air temperature were generated with the humidity generator and measured using the sensor system (figure 10).

First, an air temperature of 25 °C and a dew point temperature of 15 K below air temperature (=10 °C) were set. Then the dew point temperature was increased to 3 K and finally to 1 K below air temperature (= 22 and 24 °C, respectively). Each dew point temperature was held for 3 h and each 2 s the sensor system took a measurement value. In figure 10, each 100th measurement value is depicted. This procedure was repeated for air temperatures of 50 and 70 °C. The measurement results are listed in table 1.

It can be seen from figure 10 (crosses in the diagram, right axis) that the absolute deviations between the measured and

Table 1. Summary of the measurement results shown in figure 10.

Air temperature (°C)	Set dew point temperature (°C)	Relative humidity (calculated) (%)	Reference dew point temperature (°C)	Measured dew point temperature (°C)
25	10	38.74	10 ± 0.04	9.56 ± 0.02
25	22	83.45	22 ± 0.02	21.58 ± 0.01
25	24	94.19	24 ± 0.01	23.7 ± 0.01
50	35	45.57	35 ± 0.07	35.01 ± 0.04
50	47	86.03	47 ± 0.02	46.88 ± 0.01
50	49	95.14	49 ± 0.01	48.63 ± 0.01
70	55	50.52	55 ± 0.04	54.96 ± 0.25
70	67	87.72	67 ± 0.01	66.92 ± 0.02
70	69	95.75	69 ± 0.02	69.12 ± 0.02

reference dew point temperatures are for all air temperatures and humidity values in the range of ±0.5 K. Looking at the mean values of the measured dew point temperatures in table 1, it can be seen that the sensor system measures with a mean deviation between −0.42 °C (air temperature = 25 °C, dew point temperature = 22 °C) and +0.12 °C (air temperature = 70 °C, dew point temperature = 69 °C). The standard deviations are in the range of ±0.02 °C for most air and dew point temperature combinations. It is remarkable that at each air temperature the standard deviation is highest for the lowest dew point temperature. Overall, the results prove that the sensor system works with good accuracy at high air temperatures and at high RH values.

4.2. Characterization at low humidity

To characterize the sensor system at low dew point temperatures, a trace humidity generator (aDROP Feuchtemeßtechnik GmbH, aGE-LOW [16]) was used to generate humid air with low dew point temperatures. The investigated sensor system was equipped with a two-stage peltier cooler which enables a maximum cooling of the sensor membrane down to 45 K below ambient temperature. The measurements presented in figure 11 were carried out at an air temperature of about 22 °C.

The measurements started at a dew point temperature of 10 °C (~46.4% RH). Then, the dew point temperature was decreased to 5 °C (~33% RH), 0 °C (~23.1% RH), −10 °C (~10.8% RH) and finally −20 °C (~4.75% RH). After that, the dew point temperature was increased back to 10 °C stopping at the same intermediate values as during dew point temperature decrease. Each dew point temperature was kept constant for 3 h and the sensor system measured every 2 s. In figure 11 every 100th measurement value is shown. Because the trace humidity generator is not able to generate exactly the set dew point temperatures (especially at lower humidity values) a chilled mirror hygrometer (EdgeTech DewMaster [17]) was used for reference measurements. A summary of the measurement results is listed in table 2.

It can be seen from table 2 that for dew point temperatures between 10 and 0 °C the mean deviation between our sensor system and reference hygrometer are in the range of the accuracy of the reference hygrometer which is ±0.2 K. For lower dew point temperatures the deviations get larger. It is
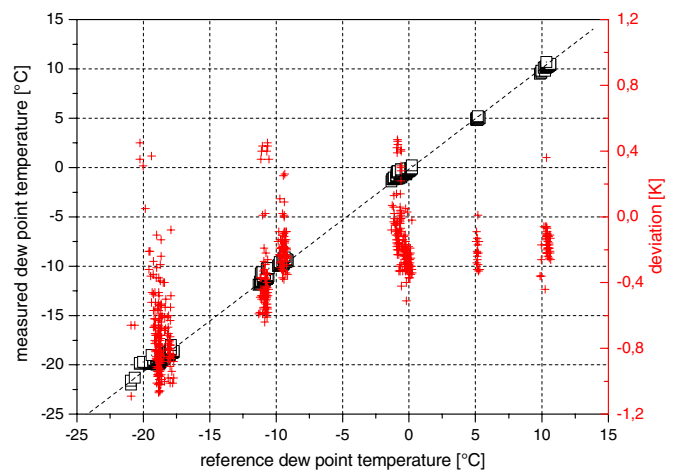
Figure 11. Measured dew point temperature compared to reference values. Humid air was generated using a trace humidity generator (aDROP Feuchtemeßtechnik GmbH, aGE-LOW [16]) at an air temperature of about 22 °C. The reference dew point temperatures on the *x*-axis are values measured using a chilled mirror hygrometer (EdgeTech DewMaster [17]). On the right axis the deviation between measured and reference dew point temperatures is shown.

remarkable that the mean measurement values of the presented sensor system are all below the mean values measured using the reference hygrometer. In particular for dew point temperatures in the range of −20 °C the deviation is in the range of nearly −1 K. As described earlier, the sensor membrane should be the coldest spot of the sensor system which is in contact with the air. In our current setup air also gets in contact with the peltier cooler which is colder than the sensor membrane. Hence, water prefers to condense and also to freeze on the surface of the peltier cooler. This might cause a local reduction of water vapor near the sensor membrane, which leads to a decrease in dew point temperature. It is assumed that this effect is more relevant for lower dew point temperatures. Nevertheless, in summary the measurements showed that the sensor system is able to measure low dew point temperatures with good accuracy.

4.3. Characterization of dynamic behavior

Two measurements at an ambient temperature of about 22 °C were carried out to characterize the dynamic behavior of

Table 2. Summary of the measurement results presented in figure 11 (air temperature ≈ 22 °C). The values given in the columns for reference and measured dew point temperatures are the mean values ± standard deviations. In column 'deviation' the mean values of the deviation between reference and measured dew point temperatures with respective standard deviation is listed.

Set dew point temperature (°C)	Relative humidity (calculated) (%)	Reference dew point temperature (°C)	Measured dew point temperature (°C)	Deviation (K)
10	46.4	10.39 ± 0.19	10.23 ± 0.24	−0.16 ± 0.1
5	33	5.16 ± 0.07	4.97 ± 0.13	−0.2 ± 0.13
0	23.1	−0.46 ± 0.38	−0.59 ± 0.33	−0.13 ± 0.2
−10	10.8	−10.12 ± 0.73	−10.38 ± 0.83	−0.26 ± 0.23
−20	4.75	−18.75 ± 0.46	−19.5 ± 0.45	−0.74 ± 0.23
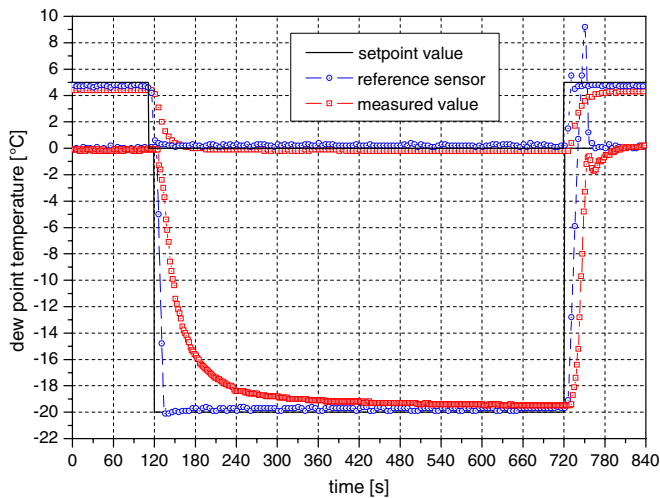
Figure 12. Time-dependent measurement values of the sensor system at rapid changes of dew point temperatures (5 °C → 0 °C → 5 °C and 0 °C → −20 °C → 0 °C) compared to reference values. Humid air was generated using a trace humidity generator (aDROP Feuchtemeßtechnik GmbH, aGE-LOW [16]) at an air temperature of about 22 °C. The reference dew point temperatures were measured using a chilled mirror hygrometer (EdgeTech DewMaster [17]).

the sensor system using a trace humidity generator (aDROP Feuchtemeßtechnik GmbH, aGE-LOW [16]). In a first measurement the dew point temperature was set to 5 °C. After 2 min it was rapidly decreased to 0 °C and increased back to 5 °C after additional 10 min (figure 12). In a second measurement the procedure was repeated starting at a dew point temperature of 0 °C, decreasing it to −20 °C, and increasing it back to 0 °C. For reference measurements a chilled mirror hygrometer (EdgeTech DewMaster [17]) was used. The presented sensor system took measurement values every 2 s.

It can clearly be seen that the presented sensor system is slower than the chilled mirror hygrometer. Particularly when the dew point temperature is decreased from 0 to −20 °C the response time is significantly higher compared to the chilled mirror hygrometer. We assume that the slow response time of our sensor system, especially when the dew point temperature is decreased, is considerably caused by condensed water on the surface of the peltier cooler (see section 4.2). When the dew point temperature is decreased, the condensed water evaporates and might cause a local enrichment of water vapor near the sensor membrane leading to an increase in measured dew point temperature. We furthermore assume that the slow response time is also caused by the control

electronics we use to drive the peltier cooler. The control parameters of the implemented PI-controller are not optimized regarding response time of the sensor system. It is remarkable that both chilled mirror hygrometer and the presented sensor system show an overshoot when the dew point temperature is rapidly increased. We assume that this is not caused by the humidity generator. Instead we think that this is caused by the sensors. Both are periodically putting out temperature values independent of whether the mirror and the sensor membrane, respectively, are at dew point temperature or not. Hence, the output values show the dynamic temperature profile of mirror and sensor membrane, respectively. In particular when the dew point temperature is increased from −20 to 0 °C both sensors need at least 40 s until they measure reasonable dew point temperature values.

5. Summary and outlook

This paper presents a dew point temperature sensor which is based on the thermal detection of condensed water on a micromachined thin membrane which is chilled by a peltier cooler. The sensor is able to measure dew point temperatures in the range of 1 K to nearly 45 K below air temperature. The presented measurement results showed that the sensor system is able to measure dew point temperatures with accuracy below ±0.2 K in a wide humidity range. Furthermore it could be proven that the sensor system is able to measure at high RH values of up to nearly 96% and at air temperatures of up to 70 °C with good accuracy. The sensor system is also able to measure low dew point temperatures down to approximately −20 °C at an air temperature of about 22 °C.

The main disadvantage of the current sensor system is the fact that the air to be measured gets in contact with the peltier cooler which is colder than the sensor membrane. To improve this, we are currently working on the monolithic integration of a peltier cooler directly into the sensor membrane. In first preliminary investigations the feasibility could be proven in principle and a temperature difference between sensor membrane and silicon bulk material of up to 7 K could be achieved. We are working on further increasing the achievable temperature difference and on the integration of this technology into the sensor system. Once this is achieved, it can be ensured that the sensor membrane is the coldest spot in the sensor system, even if additional external peltier coolers are used to decrease the overall temperature of the sensor chip. Another issue which has to be investigated is

the influence of contamination of the sensor membrane on the sensor accuracy. Although first preliminary tests showed that the sensor system properly works also outside the controlled environment of our laboratory, further work will be carried out to properly characterize the influence of particles, oil and other contaminations on the sensor membrane.

Acknowledgments

References

[1] Bentley R E 1998 *Temperature and Humidity Measurement—Handbook of Temperature Measurement* vol 1 (New York: Springer) ISBN 981-4021-09-1 pp 134ff

[2] Soloman S 2009 *Sensors Handbook* (New York: McGraw-Hill) ISBN 978-0-07-160571-7 p 704

[3] Kulwicki B 1991 Humidity sensors *J. Am. Ceram. Soc.* **74** 697–708

[4] Chen Z and Chi L 2005 *Humidity Sensors: A Review of Materials and Mechanisms (Sensor Letters* vol 3*)* (Valencia, CA: American Scientific Publishers) pp 274–95

[5] Fenner R and Zdankiewicz E 2001 Micromachined water vapor sensors: a review of sensing technologies *Sensors J. IEEE* **1** 309–17

[6] Rittersma Z M 2002 Recent achievements in miniaturised humidity sensors—a review of transduction techniques *Sensors Actuators* **96** 196–210

[7] Jachowicz R S, Weremczuk J, Paczesny D and Tarapata G 2009 MEMS based super fast dew point

[8] Sensirion AG 2011 Digital humidity sensors (RH&T)—overview (www.sensirion.com/en/01_humidity_sensors/00_humidity_sensors.htm) website accessed on 22 August 2011

[9] CiS Forschungsinstitut für Mikrosensorik und Photovoltaik GmbH 2011 Dew point measuring (www.cismst.org/en/loesungen/taupunktmessgeraete/) website accessed on 22 August 2011

[10] Lang W, Glosch H, Billat S, Querrioux T, Kunze M, Ashauer M and Sandmaier H 2003 Humidity measurement by dynamic dew-point detection *12th Int. Conf. on Solid State Sensors, Actuators and Microsystems (Boston, MA, 8–12 June 2003)* vol 2 pp 1864–6

[11] Kunze M, Glosch H, Ehrbrecht B, Billat S, Messner S, Ashauer M and Zengerle R 2007 Thermal dewpoint sensing: a new approach for dewpoint detection and humidity sensing *Proc. 20th Int. Conf. on Micro Electro Mechanical Systems IEEE* pp 119–22

[12] Ashauer M, Glosch H, Hedrich F, Hey N, Sandmaier H and Lang W 1999 Thermal flow sensor for liquids and gases based on combinations of two principles *Sensors Actuators* A **73** 7–13

[13] Isothermal Technology Limited Products 2011 (www.isotech.co.uk/category.php) website accessed on 22 August 2011

[14] Thunder Scientific Corporation 2011 Model 2500 Benchtop/Mobile—'Two-Pressure' Humidity Generator (www.thunderscientific.com/humidity_equipment/model_2500.html) website accessed on 22 August 2011

[15] Lawrence M 2005 The relationship between relative humidity and the dewpoint temperature in moist air: a simple conversion and applications *Bull. Am. Meteorol. Soc.* **86** 225–33

[16] aDROP Feuchtemeßtechnik GmbH aGE-LOW2011 (www.adrop.de /index.php?option=content&task=view&id=6&Itemid=37) website accessed on 22 August 2011

[17] EdgeTech 2011 Dewmaster chilled mirror hygrometer (www.edgetech.com/moisture-humidity/gallery/category/instrumentation) website accessed on 22 August 2011

hygrometer—construction and medical applications *Meas. Sci. Technol.* **20** 124008